Journal of Constructional Steel Research 217 (2024) 108656

Contents lists available at ScienceDirect

Journal of Constructional Steel Research

journal homepage: www.elsevier.com/locate/jcsr

Reliability analysis of shear design provisions for cold formed steel sections

L. Simwanda [a,*], P. Gatheeshgar [b], B.D. Ikotun [a], M. Bock [c], E.K. Onyari [a], F.M. Ilunga [a]

[a] Department of Civil Engineering, University of South Africa, Johannesburg, South Africa
[b] School of Computing, Engineering and Digital Technologies, Teesside University, Middlesbrough, United Kingdom
[c] School of Infrastructure and Sustainable Engineering, Aston University, United Kingdom

ARTICLE INFO

Keywords:
Cold formed steel sections
Structural reliability analysis
Shear design
EN 1993-1-3 standard
First order reliability method

ABSTRACT

This study focuses on the structural reliability analysis of cold-formed steel (CFS) sections under the ultimate limit state of shear. It considers two design models: the EN 1993-1-3 standard and its recent modification proposed by a previous study. The bias and uncertainty in these models were calibrated by comparing the design models' prediction to 67 experimental results. Reliability analyses for the CFS beams, designed according to both models, were conducted using Monte Carlo Simulation (MCS) and the First Order Reliability Method (FORM). This analysis incorporated the model uncertainty and other parameters describing these models into the stochastic description. The 10% fractile of the reliability values for beams designed using the existing EN 1993-1-3 provisions showed values that were more conservative than those of the modified EN 1993-1-3 provisions, compared to the reliability target of 3.8. A FORM sensitivity analysis identified the yield strength of steel f_{yb} and the resistance model uncertainty Γ_R as the main positive drivers of uncertainty in the computed reliability indices of the design models. Additionally, a multiplicative modification factor was proposed for both the existing and modified versions of EN 1993-1-3, ensuring that these models optimally meet the specified reliability targets of 3.8 and 4.3 for Eurocode reliability classes 2 and 3, respectively. The proposed modifications maintain the partial factor γ_{M0} at 1.0, as stipulated by the EN 1993-1-3 provisions for the resistance of the cross-section.

1. Introduction

The design of cold-formed steel (CFS) sections is a crucial aspect of structural engineering, due to their extensive use as load-bearing elements in various applications. Renowned for their high strength-to-weight ratio, these sections serve as integral elements in modern modular construction [1]. The complex shear behavior of these slender sections, under a variety of loading conditions, has been the subject of thorough research (e.g. [2–6]), informing design guidelines encompassed within various international codes such as the European EN1993-1-3 [7], the North American AISI S100 [8], and the Australasian AS/NZS 4600 [9]. It is worth noting that a study by Pham and Hancock [10] laid the ground work for the development of the direct strength method (DSM) shear design rules for in both the AISI S100 and the AS/NZS 4600 design standards. Despite the comprehensive nature of these standards, the progression of theoretical knowledge and practical applications necessitates ongoing refinement of these shear provisions.

A succession of investigative work has progressively shed light on the understanding of the shear behavior of CFS section. Initial studies by researchers like Schafer and Peköz [11] laid the foundation for understanding the buckling phenomena inherent in thin-walled structures. Subsequent in-depth examinations by Yu and LaBoube [2], Keerthan and Mahendran [3], and Pham and Hancock [6] have delved into the complex interactions at the web–flange junctures, revealing factors critically influencing shear strength. These explorations have been vital in formulating and refining shear design guidelines, with the work of Keerthan and Mahendran [3], in particular, underscoring the importance of juncture restraint on shear capacity.

Building on these benchmark studies, recent deterministic assessment, such as those conducted by Gatheeshgar et al. [12], assessed the suitability of existing Eurocode provisions. These investigations have not only highlighted the limitations in current standards but have also paved the way for proposed amendments that enhance accurate shear strength predictions [12].

Nevertheless, relying solely on deterministic methods of assessment falls short in comprehensively capturing the different characteristics of CFS behavior in real-world scenarios. This is evident due to the inherent variability in material parameters and the limited understanding of the restraint level at the web–flange juncture. Acknowledging this, the probabilistic studies by researchers such as Chaves et al. [13]

* Corresponding author.
E-mail address: simwals@unisa.ac.za (L. Simwanda).

https://doi.org/10.1016/j.jcsr.2024.108656
Received 19 December 2023; Received in revised form 5 March 2024; Accepted 30 March 2024
Available online 6 April 2024

Nomenclature

θ	Slope of the web reference to the flanges
λ_w	Relative web slenderness
$\lambda_{w,new}$	Revised relative web slenderness
γ_{M0}	Partial factor
a	Shear span
b	Flange width
v	Coefficient of variation
d_1	Clear web height
E	Elastic modulus of the material
f_{bv}	Shear strength considering the buckling into account
f_{yb}	Basic yield strength of the steel
h	Web height
h_w	Web height between midlines of the flanges
k_n	Level of restraint
k_{sf}	Shear buckling coefficients of plates with simple-fixed boundary condition
k_s	Shear buckling coefficients of plates with simple-simple boundary condition
k_v	Shear buckling coefficient
s_w	Height of the web measured between the midpoints of the corners
t	Thickness
r	Corner radius
$V_{b,Rd}$	Shear resistance
$V_{EN1993-1-3}$	Shear strength prediction from EN 1993-1-3
$V_{ModifiedEN1993-1-3}$	Shear strength prediction from modified EN 1993-1-3
V_{Test}	Shear strength from experiments
g	Performance function for reliability analysis
Γ_R	Model uncertainty for the resistance models
$\Gamma_{EN1993-1-3}$	Model uncertainty for the EN 1993-1-3 shear model
$\Gamma_{ModifiedEN1993-1-3}$	Model uncertainty for the modified EN 1993-1-3 shear model
Γ_S	Model uncertainty for the action effects
D_n	Kolmogorov–Smirnov statistic
$f_x(x)$	Probability density function
$F_x(x)$	Cumulative distribution function
μ_X	Mean of a random variable X
σ_X	Standard deviation of a random variable X
G	Permanent action
Q	Imposed variable action
γ_G	Partial factor for permanent action
γ_Q	Partial factor for imposed variable action
κ	Imposed variable action to permanent action ratio
β	Reliability index
β_T	Target reliability index
k_γ	Partial factor related modification factor
α	Importance vector

and Meimand and Schafer [14] have augmented the literature by integrating the variability of material properties into the safety assessments of cold formed elements. The pioneering work in probabilistic design by Ellingwood and Galambos [15] has also been vital in promoting a shift towards reliability-based design approaches.

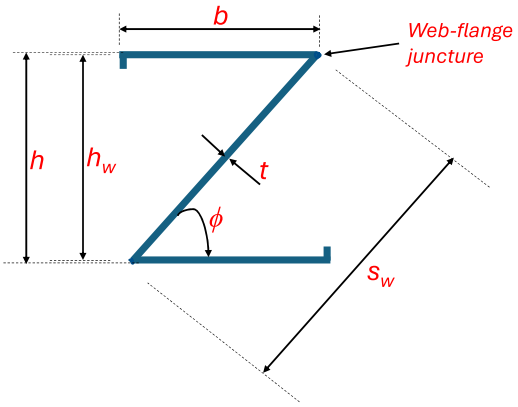

Fig. 1. General sectional configuration of a CFS section with a sloping web.

The concept of structural reliability provides a standardized metric for evaluating the safety of various structures by comparing their resistance capabilities. This approach establishes the most objective criterion for determining the safety of structures [16]. Modern structural design guidelines commonly incorporate this methodology, calibrating partial factors to ensure they meet fundamental and optimal safety requirements [17].

This work integrates the deterministic foundations laid by prior research [12] with a probabilistic approach to the shear strength assessment of shear provisions for CFS sections. By collating and analyzing experimental results from a spectrum of scholarly sources, model uncertainty in the existing EN 1993-1-3 model and the proposed modified version is calibrated. Thereafter, the structural reliability of CFS beams designed to the two considered models is computed by incorporating model uncertainty, geometric, and material uncertainty into the stochastic description of the problem. This study seeks to reinforce the deterministic rigor of existing provisions conducted by Gatheeshgar et al. [12] with the robustness required to withstand the inherent aleatory and epistemic uncertainties present in practical applications, thus proposing modifications that uphold structural integrity within a probabilistic framework [18].

2. Analysis of CFS sections under shear failure

This section outlines the analysis of shear behavior in CFS sections, incorporating both deterministic and probabilistic approaches. It begins with a deterministic analysis of shear strength as per EN1993-1-3 [7], followed by an examination of the modifications proposed by Gatheeshgar et al. [12]. The section concludes with an introduction to the performance function, a key component in reliability analysis, bridging deterministic findings with probabilistic assessments.

2.1. Existing eurocode shear design provisions

The design guidelines outlined in EN1993-1-3 contain a methodology for calculating the shear resistance in CFS elements. The design values of the shear resistance $V_{b,Rd}$ is given by the equation:

$$V_{b,Rd} = \frac{(h_w / \sin(\phi)) \cdot t \cdot f_{bv}}{\gamma_{M0}} \quad (1)$$

In Eq. (1), h_w denotes the distance between the midpoints of the flange edges, and ϕ denotes the web's angle in relation to the flanges (see Fig. 1). The variable t stands for the web thickness, while f_{bv} signifies the shear strength, accounting for the potential of buckling effects. The term γ_{M0} is the partial factor for the ultimate limit state of resistance of the cross-section.

In order to compute the shear buckling strength f_{bv}, the EN1993-1-3 recommends taking into account the web's relative slenderness λ_w and

the basic yield strength of steel f_{yb}. For webs without of longitudinal stiffeners (focus of this study), λ_w is computed via Eq. (2):

$$\lambda_w = 0.346\left(\frac{s_w}{t}\right)\sqrt{\frac{f_{yb}}{E}} \tag{2}$$

Herein, E signifies the material's modulus of elasticity, and s_w measures the web's height from the corner midpoints. EN1993-1-3 also notes that the shear buckling strength f_{bv} is a function of the presence of web stiffening at the support points. In the experiments considered for the calibration of model uncertainty in Section 3.1, stiffening was typically achieved by affixing cleat plates or side plates to the web, which served to mitigate web distortion and effectively resist support reactions. For scenarios with web stiffening at the supports, EN1993-1-3 proposes the following formulae to approximate the shear buckling strength f_{bv}:

$$f_{bv} = \begin{cases} 0.58 f_{yb} & \text{when } \lambda_w \le 0.83 \\ \frac{0.48 f_{yb}}{\lambda_w} & \text{when } \lambda_w > 0.83 \end{cases} \tag{3}$$

2.2. Modified eurocode shear design provisions

The current shear design guidelines in EN1993-1-3 have limitations, particularly in accounting for the web–flange juncture restraint level and the aspect ratio [12]. Gatheeshgar et al. [12] proposed an enhanced approach to integrate these factors into the Eurocode's shear design rules. This approach introduces a new formula for calculating the modified web slenderness, denoted as $\lambda_{w,\text{new}}$, as shown in Eq. (4). This new formula incorporates a novel shear buckling coefficient, k_v, allowing the incorporation of the level of restraint at web–flange juncture and aspect ratio into the formulation.

$$\lambda_{v,new} = \frac{0.735}{\sqrt{k_v}}\left(\frac{s_w}{t}\right)\sqrt{\frac{f_{yb}}{E}} \tag{4}$$

Following the approach of Lee et al. [19], Keerthan and Mahendran [4] k_v is computed as shown in Eq. (5), where k_{ss} and k_{sf} represent shear buckling coefficients under simple-simple and simple-fixed conditions, respectively. The factor k_n quantifies the restraint level at the web–flange juncture, with values assigned as 23% for lipped channel sections ($k_n = 0.23$) and 87% for hollow flange sections ($k_n = 0.87$). Eqs. (6) and (7) detail the computation of k_{ss} and k_{sf}, which are influenced by the aspect ratio, the ratio of shear span (a) to clear web height (d_1).

$$k_v = k_{ss} + k_n(k_{sf} - k_{ss}) \tag{5}$$

$$k_{ss} = \begin{cases} 4 + 5.34\left(\frac{a}{d_1}\right)^2 & \text{for } \frac{a}{d_1} < 1 \\ 5.34 + 4\left(\frac{a}{d_1}\right)^2 & \text{for } \frac{a}{d_1} \ge 1 \end{cases} \tag{6}$$

$$k_{sf} = \begin{cases} 5.34\left(\frac{a}{d_1}\right)^2 + 2.31\frac{a}{d_1} - 3.44 + 8.39\frac{a}{d_1} & \text{for } \frac{a}{d_1} < 1 \\ 8.98 + 5.61\left(\frac{a}{d_1}\right)^2 - 1.99\left(\frac{a}{d_1}\right)^3 & \text{for } \frac{a}{d_1} \ge 1 \end{cases} \tag{7}$$

This updated methodology calculates shear buckling strength f_{bv} for sections with web stiffening at the support as illustrated in Eq. (8). Notably, the analysis of experimental data reveals an inelastic reserve for small web slenderness values. Hence, for $\lambda_{w,\text{new}}$ less than or equal to 0.83, a linear trend reflecting this reserve is considered.

$$fbv = \begin{cases} (-0.22\lambda_{w,\text{new}} + 0.77) f_{yb} & \text{for } \lambda_{w,\text{new}} \le 0.83 \\ \frac{0.48 f_{yb}}{\lambda_{w,\text{new}}} & \text{for } \lambda_{w,\text{new}} > 0.83 \end{cases} \tag{8}$$

The revised approach is noteworthy for its inclusion of aspect ratio and web–flange juncture constraints, factors critical to accurately determining shear response [12], particularly in CFS sections without longitudinal stiffeners and with web stiffening at the support.

2.3. Performance function

The demarcation of the failure region is a prerequisite for performing reliability analysis, enabling the distinction between safety and failure conditions. In line with the Eurocode 0 (EN 1990 [17]) standards, the performance function for the ultimate limit state of shear buckling of CFS channels is formulated in Eq. (9), inclusive of parameters representing model error (also known as model uncertainty) on both the resistance and action variables.

$$g = \Gamma_R \cdot V_{b,Rm} - \Gamma_S \cdot (V_{Dm} - V_{Lm}) \tag{9}$$

In this expression, Γ_R and Γ_S encapsulate the stochastic variables that characterize the model uncertainty associated with shear strength of CFS sections and applied shear actions, respectively. $V_{b,Rm}$ is the shear buckling resistance computed at the mean values of geometric and material parameters, while V_{Dm} and V_{Lm} symbolize the permanent and imposed variable action effects of the applied shear action, taken also at their mean values. The Subsequent section will present the uncertainty quantification of the stochastic variables involved in this performance function.

3. Uncertainty quantification

This section delves into the uncertainty quantification of stochastic variables and models relevant to the study's reliability analysis. Given the inherent lack of complete and precise data for all input variables in a typical engineering problem, it becomes imperative to use probabilistic models to encapsulate the uncertainties in these variables. The analysis specifically considers uncertainties in sectional dimensions, material properties, and the predictive models used for calculating ultimate shear strength of CFS sections.

3.1. Model uncertainty for shear resistance

In addressing the unpredictability inherent in engineering problems, it is essential to acknowledge that complete and precise data for all input variables is often unattainable [20]. Consequently, probabilistic models become indispensable tools for encapsulating uncertainties in these variables, particularly in the context of reliability analysis [20]. This analysis focuses on the uncertain aspects of sectional dimensions, material properties, and predictive models used for ultimate strength estimation.

Model uncertainties arise primarily from the design equations used to forecast ultimate strength, which are based on a series of hypotheses and approximations. As a result, the estimation of potential model errors becomes a crucial aspect of ensuring the accuracy and reliability of these predictive models. In many cases of reliability analysis, one of the fundamental steps involves identifying and quantifying these modeling uncertainties [21]. In this study, the model uncertainty for the resistance variable is denoted as Γ_R and is conceptualized as the discrepancy between experimental results, $V_{b,R}^{\text{expt}}$ and model predictions, $V_{b,R}^{\text{pred}}$ computed using Equations described in Sections 2.1 and 2.2, as provided in Eq. (10),

$$\Gamma_R = \frac{V_{b,R}^{\text{expt}}}{V_{b,R}^{\text{pred}}} \tag{10}$$

To statistically characterize Γ_R, statistical moments such as mean μ and standard deviation σ are computed over a sample or an experimental design of Γ_R. To gather statistical data on Γ_R, information from 67 CFS beams was compiled from multiple sources [22–27]. Among these, 23 were hollow flange sections (Litesteel beam) and remaining 34 were lipped channel sections. Fig. 2 in the study illustrates the variation of $\Gamma_{\text{EN1993-1-3}}$ and $\Gamma_{\text{Modified EN1993-1-3}}$ as a function of the relative web slenderness λ_w and revised relative web slenderness $\lambda_{w,\text{new}}$, respectively. Further details about this aggregated data are available in Table 1.

Table 1
Statistical data of model uncertainty (Γ_R) for CFS channels subjected to shear.

References	No. of specimens	$\Gamma_{\text{EN1993-1-3}}$		$\Gamma_{\text{Modified EN1993-1-3}}$	
		μ	σ	μ	σ
Keerthan and Mahendran [22]	23	1.47	0.21	1.01	0.07
Keerthan and Mahendran [23]	15	1.38	0.19	0.98	0.09
Pham and Hancock [24]	18	1.49	0.21	1.03	0.09
Chen et al. [25]	4	1.27	0.18	0.90	0.09
Pham et al. [27]	4	1.50	0.16	1.09	0.10
Pham et al. [26]	3	1.39	0.06	1.10	0.05

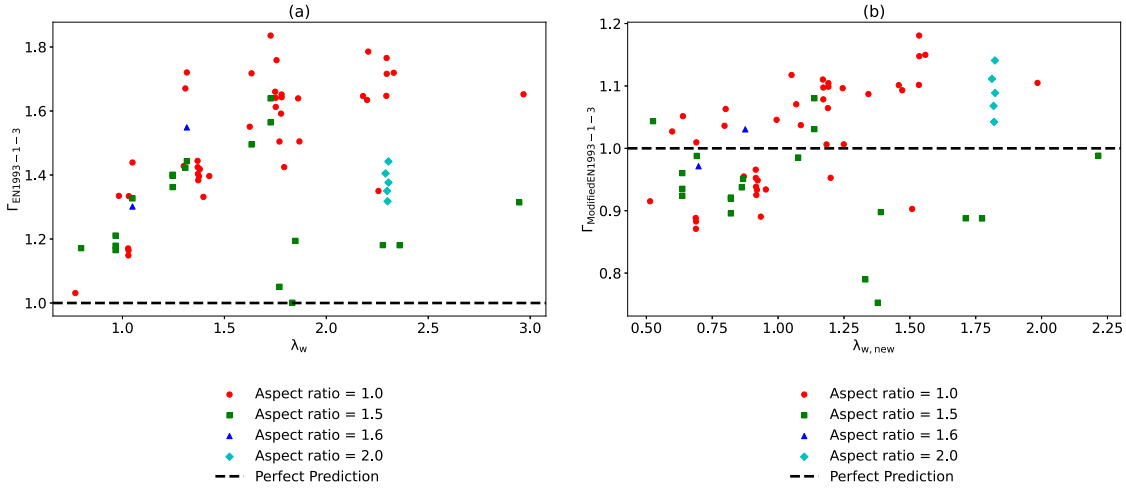

Fig. 2. Comparison between model error Γ_R and perfect prediction as a function of λ_w and $\lambda_{w,\text{new}}$, for the (a) EN 1993-1-3 and (b) modified EN 1993-1-3 shear provisions, respectively, for CFS channels with different aspect ratios in the collected database.

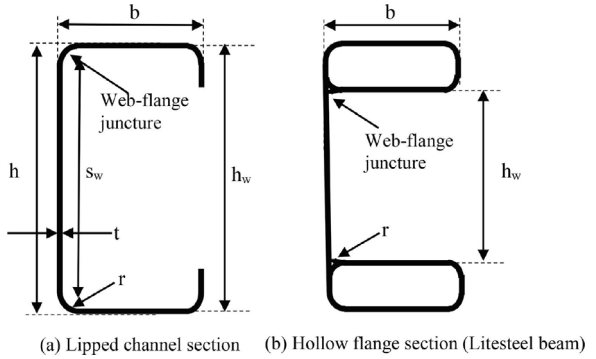

Fig. 3. Sectional configuration of the CFS sections and the notations used for the different geometric parameters.
Source: Adapted from Gatheeshgar et al. [12].

Additionally, the sectional configuration of the experimental CFS beams beam is depicted in Fig. 3.

To ascertain the distribution functions representing model errors in the two analytical models being considered, this investigation employed the Kolmogorov–Smirnov (K–S) statistic [28]. The K–S test is proficient at assessing the conformity of empirical data to a specified probability distribution, with a pronounced efficiency for normal distributions [29,30]. It encompasses a non-parametric test that deliberately avoids assumptions about the underlying distribution, allowing for a versatile evaluation of sample populations against continuous probability distribution functions [31].

Typically, the K–S statistic D_n is determined by the equation:

$$D_n = \sup_x |F_n(x) - F(x)| \tag{11}$$

where $\sup_x$ is the supremum of the set of distances, $F_n(x)$ is the empirical cumulative distribution function of the sample, and $F(x)$ is the theoretical cumulative distribution function (CDF) of the reference distribution. The critical values for the K–S statistic, which indicate the significance of the results, are well-established in the statistical domain [32]. For this analysis, the significance level was set at 5% [33], an effective threshold for a wide array of data distributions, including those with tail-end deviations [34].

Complementary to the K–S test, the p-value was computed to yield an intuitive gauge for the statistical hypotheses at play. This index, predicated on the null hypothesis, streamlines the decision-making process concerning its rejection [35]. A substantial p-value indicates a robust alignment between the posited and the actual distributions [36]. The inquiry pinpointed that all the three distributions (normal, lognormal and gamma) with specified parameters (Tables 2 and 3) most suitably captures the uncertainties for shear failure of CFS sections. The corresponding graphical representations for these probability distributions in terms of joint probability density function (PDF), and CDF are illustrated in Figs. 4 and 5. The findings from the K–S tests and the associated p-values, and the statistical moments of the model uncertainty for the EN 1993-1-3 and modified EN 1993-1-3 models are documented in Tables 2 and 3, respectively. The study adopts the lognormal distribution, along with its associated statistical moments, to represent the uncertainty of model uncertainty in accordance with the recommendations of the Joint Committee on Structural Safety (JCSS) probabilistic model code [37]. This distribution, alongside its statistical moments is then used in the subsequent reliability analyses for incorporating model uncertainty.

3.2. Materials and geometric uncertainties

3.2.1. Statistical characteristics of material parameters

Cold-formed steel's material properties, including yield strength f_y and elastic modulus E, exhibit variations due to several factors. These factors include inherent material variability stemming from the use of various steel alloys in production. Manufacturing processes

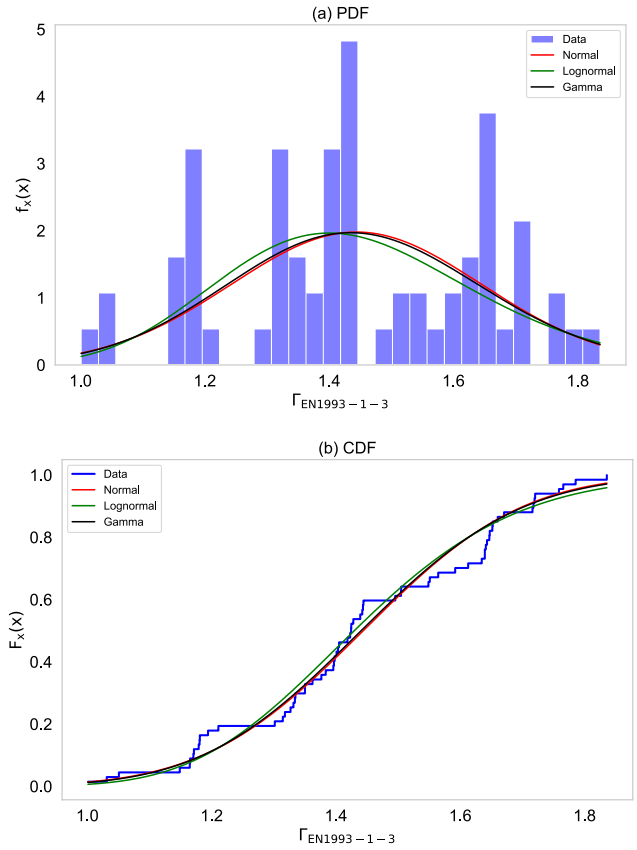

Fig. 4. Probability distributions of model uncertainty for the EN 1993-1-3 model.

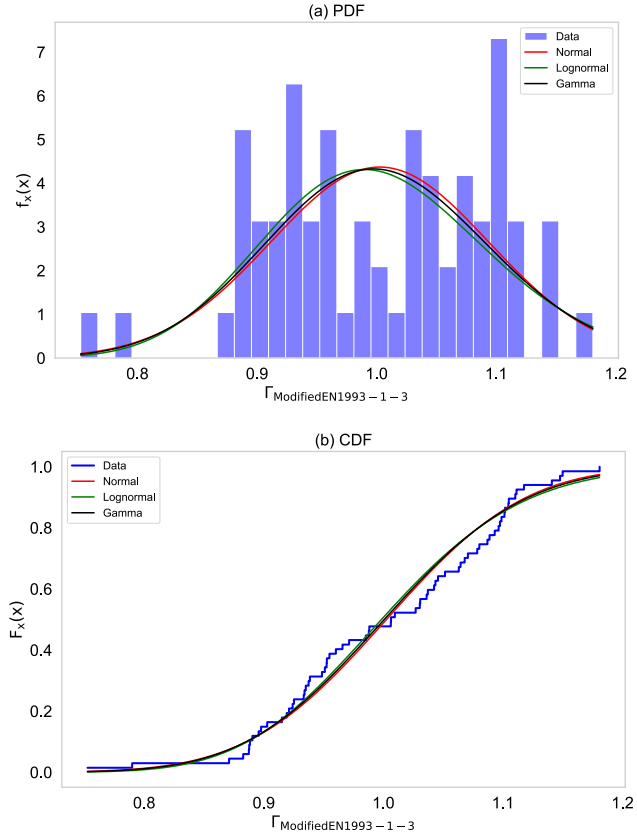

Fig. 5. Probability distributions of model uncertainty for the modified EN 1993-1-3 model.

Table 2
Results of the considered distributions of the model error for shear buckling of the EN1993-1-3 model.

Distribution	p-value	D_n	μ	σ
Normal	0.34	0.11	1.44	0.20
Lognormal	0.34	0.11	1.44	0.21
Gamma	0.35	0.11	1.44	0.21

Table 3
Results of the considered distributions of the model error for shear buckling of the modified EN1993-1-3 model.

Distribution	p-value	D_n	μ	σ
Normal	0.62	0.09	1.00	0.10
Lognormal	0.60	0.09	1.00	0.10
Gamma	0.60	0.09	1.00	0.10

Table 4
Stochastic data for material properties.

Reference	Dimension	Unit	Distribution	μ	σ
jcs [37]	f_{yb}	MPa	Lognormal	$f_{yb,k} \cdot \exp(-u, v) - C$	$0.07 \cdot \mu_{f_{yb}}$
jcs [37]	E	MPa	Lognormal	E_k	$0.03 \cdot \mu_E$

- Subscript (k) is used in Eurocode to denote characteristic value for variable under consideration.
- α is spatial position factor ($\alpha = 1.05$ for webs of hot rolled sections and $\alpha = 1$ otherwise).
- u is found to be in the range of -1.5 to -2.0.
- C is taken at a recommended value of 20 MPa.
- v is the coefficient of variation taken as 7%.

involved in the cold-forming can also introduce deviations from design assumptions. Inconsistent quality control measures during production and environmental factors during storage, transport, and handling can further influence mechanical properties. Variability in testing and certification procedures can contribute to differences between assumed and actual properties. The JCSS model code [37] addresses uncertainty by incorporating the lognormal PDF. Table 4 contains data extracted from JCSS, specifying the mean and standard deviation of the PDF for the two random variables.

3.2.2. Statistical characteristics of dimensions

The discrepancy between nominal and as-built dimension values was employed as the error variable for statistical investigation. In accordance with the JCSS probabilistic model guidelines [37], the deviation of a dimension, denoted as X, is defined as the difference between its statistical deviation characteristic, represented as Y, and the nominal value X_{nom}. As per the JCSS guidelines [37], preliminary findings for steel profiles suggest that the mean and standard deviation of Y for fundamental dimensions (such as height, width, and thickness) are less than 1 mm. Since cold-formed sections are somewhat 10 times thinner than hot-rolled sections, a tolerance deviation of 0.1 mm between mean and characteristic value of dimensions is reasonable. Table 5 displays the statistical models for geometric parameter variations. These statistical models are utilized for subsequent reliability analysis. It is worth noting, however, that while JCSS does not provide probabilistic models for cold-formed steel, this study reasonably adopts probabilistic models for that the JCSS recommends for hot-rolled steel by adjusting these tolerance deviations to account for the differences in thickness of dimensions between hot-rolled and cold-formed steel sections. As shown in Fig. 6, the probability density functions (PDFs) illustrate the distribution of different dimensions with their corresponding mean (μ) and standard deviation (σ) values. The mean μ values are extracted as minimum values of the dataset in Table 7, and the standard deviation σ values are extracted from Table 5.

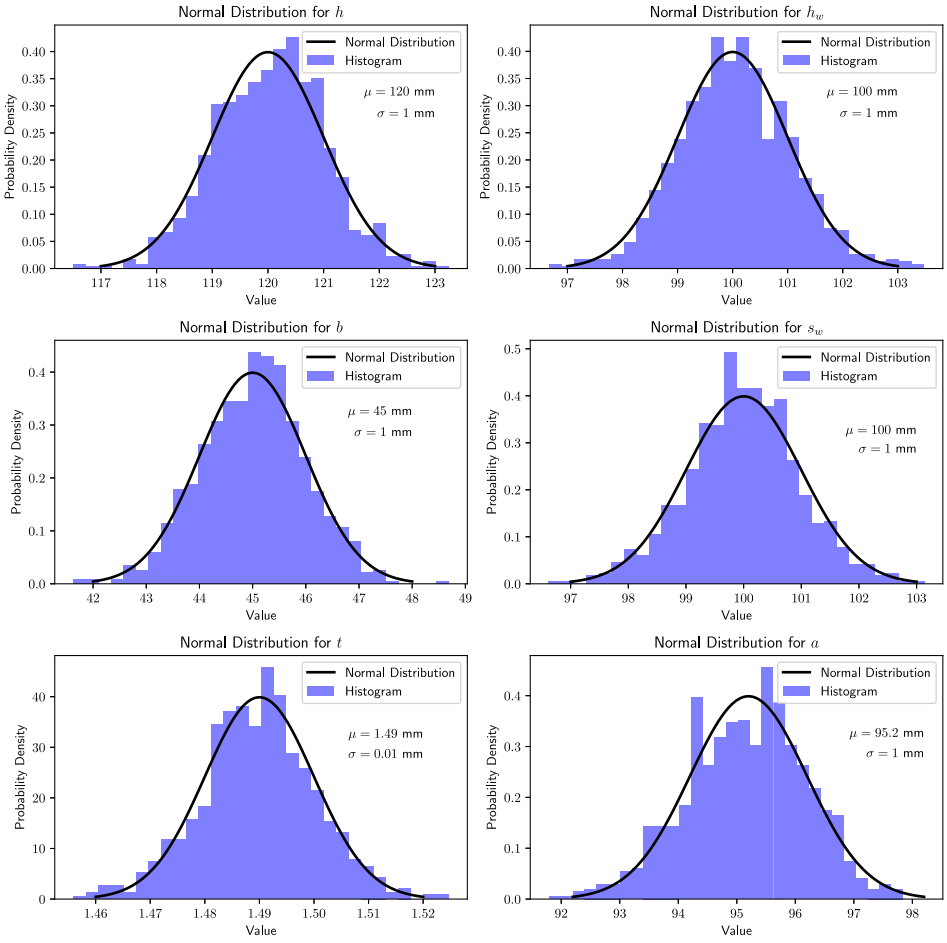

Fig. 6. Probability density functions (PDFs) for different dimensions with Mean (μ) and Standard Deviation (σ) Values. Each subplot represents a normal distribution curve fitted to the respective dimension, with mean μ values extracted as minimum values of the dataset in Table 7 and σ values extracted from Table 5.

Table 5
Stochastic data for geometric dimensions.

Reference	Dimension	Unit	Distribution	μ	σ
jcs [37]	h	mm	Normal	$h + 0.1$	1.0
jcs [37]	h_w	mm	Normal	$h_w + 0.1$	1.0
jcs [37]	b	mm	Normal	$b + 0.1$	1.0
jcs [37]	s_w	mm	Normal	$s_w + 0.1$	1.0
jcs [37]	t	mm	Normal	$t + 0.1$	0.01
	ϕ	rad.	Constant	ϕ	–
jcs [37]	a	mm	Normal	$a + 0.1$	1.0
jcs [37]	d_1	mm	Normal	$d_1 + 0.1$	1.0

Table 6
Statistical data of loads.

Load type	Bias	CoV	Distribution
G	1.05	0.1	Normal [40]
Q	1	0.25	Gumbel [40]

3.3. Action uncertainties

When designing a CFS section using the limit state design philosophy outlined in EN 1990 [17], two categories of actions affecting the CFS beam are considered: permanent G and variable Q actions. The permanent action is largely due to the self-weight of the structure, with a high degree of predictability, often modeled as a normally distributed variable [38,39]. The variable action, which takes into account the presence and movement of individuals and objects within the structure, displays variability based on the size of the area they influence; an increase in area typically leads to a reduction in action intensity. Specific statistical models for these actions are adopted from authoritative literature [40] and the information is listed in Table 6.

Adhering to the guidelines of Turkstra's rule [38], the analysis typically holds the permanent action as a baseline and factors in the peak of the variable action for action combinations. This approach is grounded in the rationale that the simultaneous peaking of multiple actions has a probability of occurrence approximately zero. Eqs. (12)–(14) establish a framework for computing the design actions. The idea is to combine the adjusted permanent and variable actions, which are essential for the structural design process, ensuring that the structural component can withstand both expected and unexpected forces throughout its design life.

$$E_d = \gamma_G V_G + \gamma_Q V_Q \tag{12}$$

Herein, V_G and V_Q are the characteristic values of permanent and variable actions, respectively, with value are calculated using the following equations,

$$V_G = \frac{V_{Ed}}{(\gamma_G + \gamma_Q \cdot \kappa)} \tag{13}$$

$$V_Q = \frac{\kappa V_{Ed}}{(\gamma_G + \gamma_Q \cdot \kappa)} \tag{14}$$

where V_{Ed} is the design value for shear capacity considering the partial factor γ_{M0}, and $\kappa = \frac{V_Q}{V_G}$ is the ratio of the characteristic variable action to the characteristic permanent action. Moreover, γ_G and γ_Q were taken 1.35 and 1.5, respectively [41].

4. Reliability analysis

Reliability analysis, a branch of probability theory, addresses uncertainties at the level of both epistemic and aleatory, in engineering using mathematical methods, facilitating real-world safety evaluations and aiding in risk informed design decisions [39]. Reliability problems are typically solved by representing uncertainty in parameters via a random vector $\mathbf{x}$ following some joint PDF $f_{\mathbf{x}}(\mathbf{x})$ and then defining the so called performance function g. A positive value of this function indicates a safe state, while a negative value represents failure. The performance function, as expressed in Eq. (9) in detail, is generally written as:

$$g(\mathbf{x}) = R(\mathbf{x}) - S(\mathbf{x}) \tag{15}$$

where $R(\mathbf{x})$ represents the resistance variable, and $S(\mathbf{x})$ denotes the action variable, both of which are functions of random variables. The failure probability is calculated via the multi-dimensional integral:

$$p_f = \int_{D_{\mathbf{x}}} \mathbb{1}_{D_f}(\mathbf{x}) f_{\mathbf{x}}(\mathbf{x}) d\mathbf{x} = \mathbb{E}[\mathbb{1}_{D_f}(\mathbf{x})] \tag{16}$$

where $f_{\mathbf{x}}(\mathbf{x})$ is the joint PDF of random variables $\mathbf{x}$, and $\mathbb{1}_{D_f}(\mathbf{x})$ is the indicator function indicating failure,

$$\mathbb{1}_{D_f}(\mathbf{x}) = \begin{cases} 1 & \text{for } g(\mathbf{x}) \le 0 \\ 0 & \text{for } g(\mathbf{x}) > 0, \mathbf{x} \in D_{\mathbf{x}} \end{cases} \tag{17}$$

In the context of structural reliability for civil engineering applications, it is common to assess the probability of failure p_f over the expected service life of a structure, typically set at 50 years [18,37]. These failure probabilities are generally of a magnitude within the range of 10^{-3} to 10^{-4}. For a more nuanced analysis, these probabilities are often translated into their standard normal counterparts, referred to as the reliability index [16,42]. The reliability index, denoted as β, is defined through the inverse standard normal CDF, Φ^{-1}, such that β is equal to the negative inverse of the CDF evaluated at the failure probability p_f, i.e., $\beta = -\Phi^{-1}(p_f)$, where Φ symbolizes the standard normal CDF.

4.1. Reliability methods

Direct evaluation of the multiple integral in Eq. (16) is challenging, so approximate and simulation methods are often used. The analytical evaluation of the performance function g via closed-form expressions, that is Eqs. (1)–(3) and Eqs. (4)–(8), facilitate the execution of Monte Carlo simulations (MCS), which with a sufficient number of iterations, can accurately estimate the failure probability p_f. Moreover, this study also examines the application of the First Order Reliability Method (FORM). Extensive discussions on both methods are available in the body of structural reliability [43,44]. The forthcoming section provides only the critical details foundational to the reliability analyses conducted and discussed in Section 5.

4.1.1. Monte Carlo simulation (MCS)

When MCS is executed with an adequately large number of trials N, a robust estimation of the failure probability p_f can be attained. This method reinterprets Eq. (16) to calculate the expected value of the indicator function $1_{D_f}(\mathbf{x})$. An ample sample size, for instance $N = 10^7$, is utilized, consisting of independent and identically distributed sample vectors $\mathcal{X} = \{\mathbf{x}^{(1)}, \mathbf{x}^{(2)}, \ldots, \mathbf{x}^{(N)}\}$ from the joint PDF $f_{\mathbf{x}}$ of the random variables. The expected value of the indicator function with respect to $f_{\mathbf{x}}$ is then approximated by the sample mean of $1_{D_f}(\mathbf{x})$, thereby providing an estimate for p_f as:

$$\hat{p}_f^{MC} = \frac{1}{N} \sum_{k=1}^{N} 1_{D_f}(\mathbf{x}^{(k)}) = \frac{N_{\text{fail}}}{N} \tag{18}$$

where N_{fail} is the number of samples that satisfy $g \le 0$. Consequently, the associated reliability index β_{MCS} can be deduced as:

$$\beta_{MCS} = -\Phi^{-1}(\hat{p}_f). \tag{19}$$

4.1.2. First order reliability method (FORM)

FORM condenses the multivariate probability problem into a univariate format by assuming that the performance equation is linear when projected onto the standard normal space. It calculates the nearest point on this linear approximation to the origin of the standard normal space [16,42]. The Euclidean distance from this origin to the design point, denoted as u^*, quantifies the reliability index β_{HL}. The design point u^* is defined as the point in the transformed standard normal space that minimizes the distance to the origin while simultaneously satisfying the failure condition $g(u(\mathbf{x})) \le 0$.

The variable u represents the transformed variables in the standard normal space, derived from the physical space variables $\mathbf{x}$ through an isoprobabilistic transformation. This transformation typically involves normalizing the original variables $\mathbf{x}$ to have zero mean and unit variance. The failure probability p_f is then deduced from the reliability index as $p_f = \Phi(-\beta_{HL})$, where Φ is the cumulative distribution function of a standard normal distribution.

4.2. Design building set

To conduct a comprehensive reliability analysis, it is essential to gather a diverse collection of design examples that cover a wide range of potential conditions encountered in practical applications. In this study, a dataset comprising 67 experimental shear strength results for CFS sections is compiled. This dataset served as the basis for calibrating mode uncertainty in Section 3.1.

The 67 experimental shear strength results are set in this study as a set of design cases. For each CFS beam in this dataset, the characteristic imposed action required to make each CFS beam to critical under shear is adjusted . In other words, the characteristic load required to reach the limit state design for each CFS beam is determined. Subsequently, the corresponding mean imposed action for each case is computed, taking into account the coefficient of variation provided in Table 6. It is worth noting that since the beams in the database were specifically tested to fail in shear, cases where flexure or other failure modes dominate to significantly impact the computed reliability indices are not expected. In Table 7, summary statistics of the database is given, including the range considered for various parameters such as aspect ratio, web height, thickness, and yield strength.

5. Reliability results

Figs. 7 and 8 illustrate how the distribution of the reliability index β changes with increasing values of κ for both the current and modified EN 1993-1-3 models, according to calculations using the FORM. Additionally, the β values calculated by FORM closely match those determined by crude MCS, as evidenced in Table 8 for $\kappa = 1.0$, with a mean absolute percentage error (MAPE) averaging 0.87%. This finding suggests that FORM's linear approximation of the performance function is appropriate for the present reliability problem.

In Figs. 7 and 8, one can observe a positive correlation between the reliability index β and the relative web slenderness parameter λ_w. The correlation appears to be more pronounced for the original EN 1993-1-3 model than for the modified version. This difference may stem from the fact that the original EN 1993-1-3 does not consider the level of restraint at the web–flange juncture and the aspect ratio when computing the web slenderness λ_w, resulting in a less robust reliability assessment compared to the modified version.

According to EN 1990 [17], a reliability target β_T of 3.8 is recommended for structures under reliability class (RC) 2, into which most structural elements are categorized. In reliability studies, it is standard practice to measure against this RC2 benchmark. These reliability targets are established through optimization to strike a balance between safety and economic efficiency, facilitating cost-effective structural design. As evidenced in Figs. 7 and 8, the modified EN 1993-1-3 model tends towards more economically optimal designs than the existing EN 1993-1-3, which yields overly conservative designs with β values significantly exceeding 3.8.

Table 7
Summary statistics of parameters in building design set.

	Min	Q_{25}	Median	Q_{75}	Max	Mean	Std	CoV
Web height (h in mm)	120.00	153.41	200.00	204.61	300.00	197.68	44.58	0.23
Flange width (b in mm)	45.00	55.00	65.00	75.00	151.34	65.27	16.32	0.25
Web thickness (t in mm)	1.49	1.53	1.90	1.97	2.51	1.88	0.34	0.18
Clear web height (d_1 in mm)	95.20	150.00	197.00	200.00	289.60	183.17	44.53	0.24
Aspect ratio (a/d_1)	1.00	1.00	1.00	1.50	2.00	1.23	0.32	0.26
Yield strength (f_{yb} in MPa)	271.00	443.30	483.49	532.50	541.13	465.74	76.32	0.16
Elastic modulus (E in GPa)	200.00	200.00	200.00	206.90	206.90	202.34	3.13	0.02
Test shear capacity (V_b in kN)	37.50	52.85	59.50	86.29	143.70	70.55	26.30	0.37

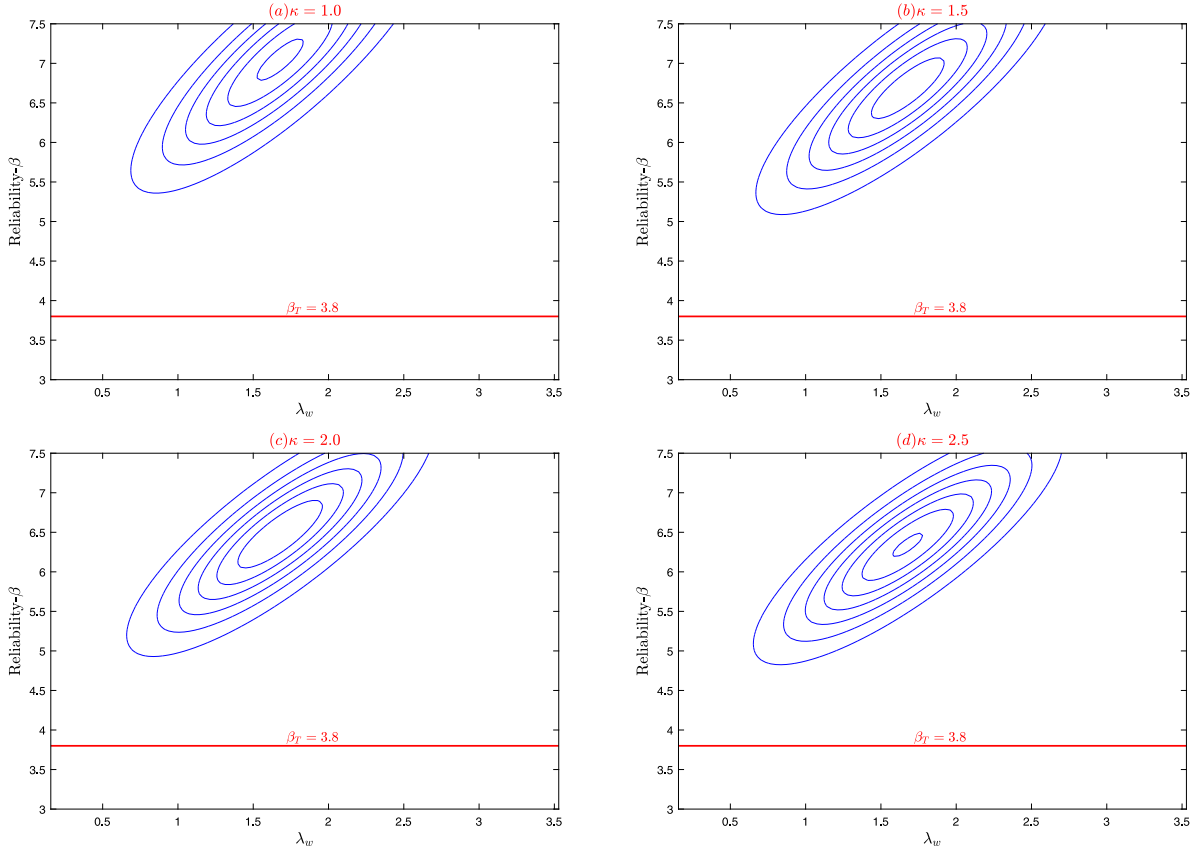

Fig. 7. Variations of distribution of the reliability index with relative web slenderness λ_w when the existing EN 1993-1-3 model is used for design.

Table 8
Computed 10% fractile of the reliability indices at $\kappa = 1.0$.

Design model	Method	μ_β	$\text{MAPE}_{\text{FORM}}$
EN 1993-1-3	FORM	5.75	1.03%
	MCS	5.81	
Modified EN 1993-1-3	FORM	4.26	0.70%
	MCS	4.29	

5.1. Sensitivity analysis based on FORM

One of the key merits of FORM analysis lies in its proficiency to pinpoint the variables that predominantly influence the computed β values. This is achieved via an importance vector of sensitivity coefficients, denoted as $\boldsymbol{\alpha}$, which quantifies the impact of each variable. This is done by approximating the performance function $g(\mathbf{x})$ near the design point with a linear function $\hat{g}(\mathbf{x}) = \|\nabla G\|(\beta - \boldsymbol{\alpha}^{\mathrm{T}}\mathbf{x})$, so that the variance of this linear approximation is given by:

$$Var[\hat{g}] = \nabla g^{\mathrm{T}} \Sigma_{xx} \nabla g = (\|\nabla g\|_{\boldsymbol{\alpha}})^2 \tag{20}$$

where $(\|\nabla g\|_{\boldsymbol{\alpha}})^2 = \|\nabla g\|^2(\alpha_1^2 + \alpha_2^2 + \cdots + \alpha_n^2)$. This signifies that the magnitude of $\|\boldsymbol{\alpha}_i\|$ reflects the variable's importance to the performance function. Variables with a larger $\|\boldsymbol{\alpha}_i\|$ are considered more critical to the considered model when used in reliability analyses.

Furthermore, the sign of each α_i is indicative of its nature. In the Eurocode [17], negative α_i corresponds to action variables, and positive α_i is related to resistance variables. The components of $\boldsymbol{\alpha}$ are determined by the sensitivity of the reliability index β with respect to the standardized random variables $\mathbf{x}$, expressed as:

$$\alpha_i = \frac{\partial \beta}{\partial x_i} \tag{21}$$

Empirical values of $\boldsymbol{\alpha}$ provided in the EN 1990 [17] give a guidance on the recommendations for variables associated with the present shear failure of CFS sections, for the EN 1993-1-3 and modified EN 1993-1-3 models as shown in Figs. 9 and 10, respectively.

Based on both the EN 1993-1-3 and the modified EN 1993-1-3 models (refer to Figs. 9 and 10), the resistance random variable Γ_R is the most influential on the computed reliability indices, followed by the yield strength of steel f_{yb}. The remaining resistance variables display

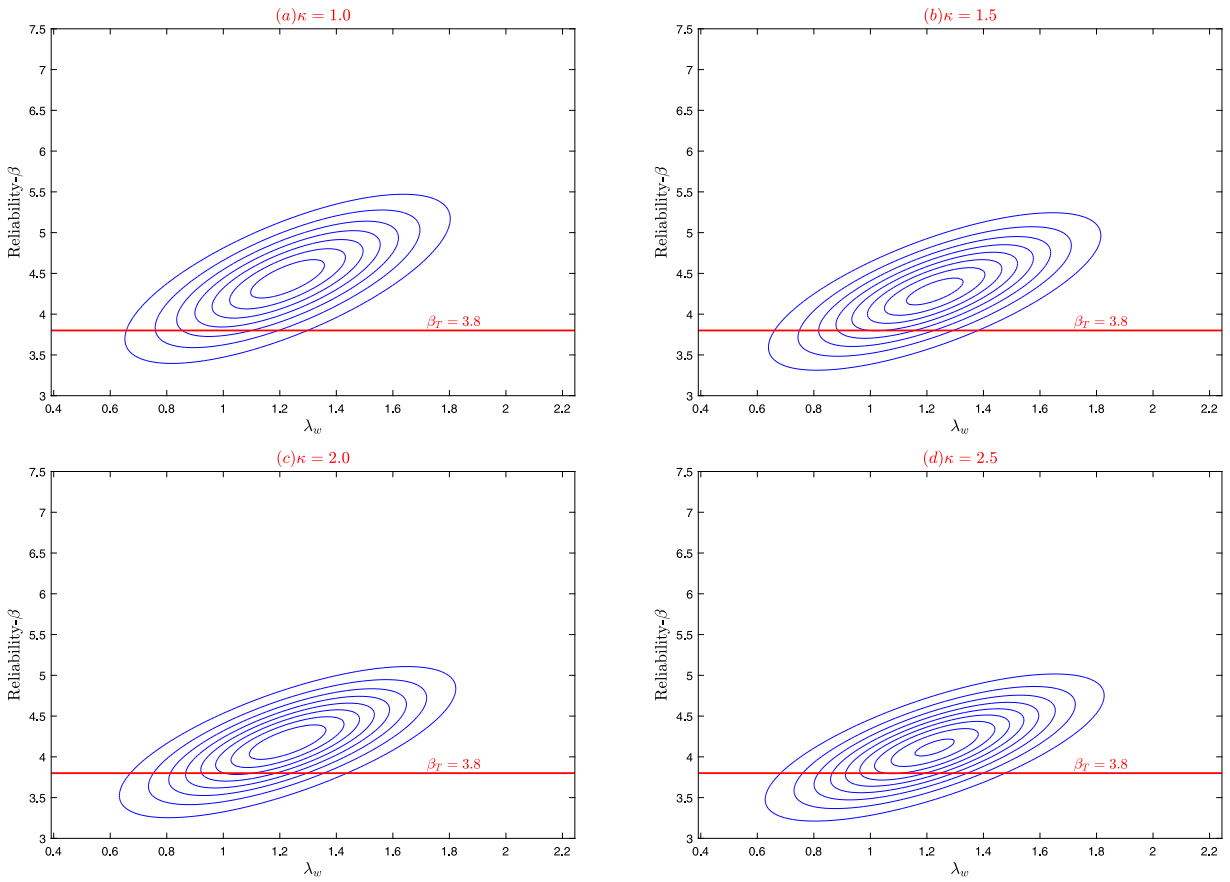

Fig. 8. Variations of distribution of the reliability index with modified relative web slenderness $\lambda_{w,new}$ when the modified EN 1993-1-3 model is used for design.

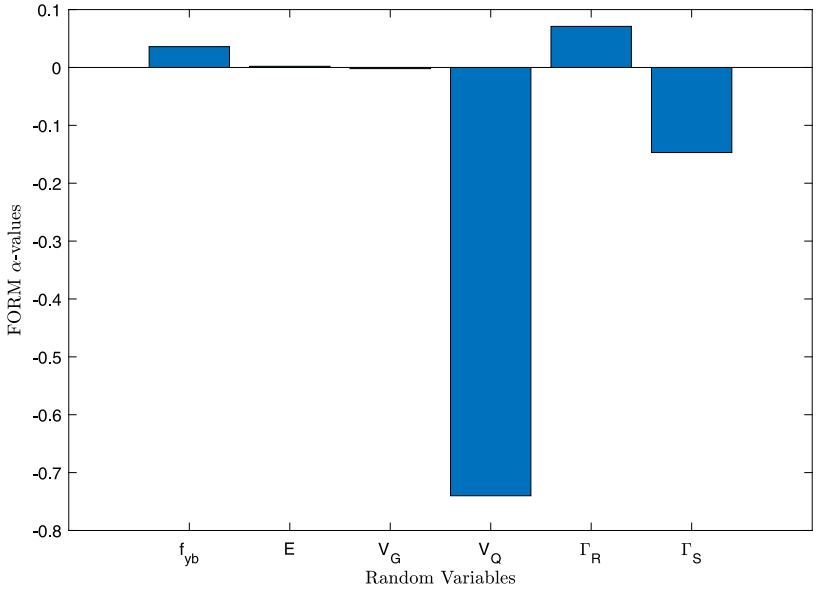

Fig. 9. Mean FORM importance vector α components for reliability analyses conducted using the EN 1993-1-3 model.

α values close to zero, suggesting that considering these variables as deterministic would be adequate in reliability calculations. Regarding action effects, the data indicate that the imposed variable action V_Q has the largest impact on the computed reliability indices, followed by the model uncertainty for action effects Γ_S. In terms of absolute value, V_Q is the most significant variable affecting the overall uncertainty in the reliability problems addressed in this study.

5.2. Reliability results based on the partial factor γ_{MO}

The impact of varying the partial factor γ_{M0} on the reliability index warrants considerable attention. The calculated 10% fractile reliability values at $\gamma_{M0} = 1.0$ seem overly conservative when compared to the optimal reliability target of $\beta_T = 3.8$, as indicated by the results in Table 8. Given budgetary constraints, such high conservatism is not

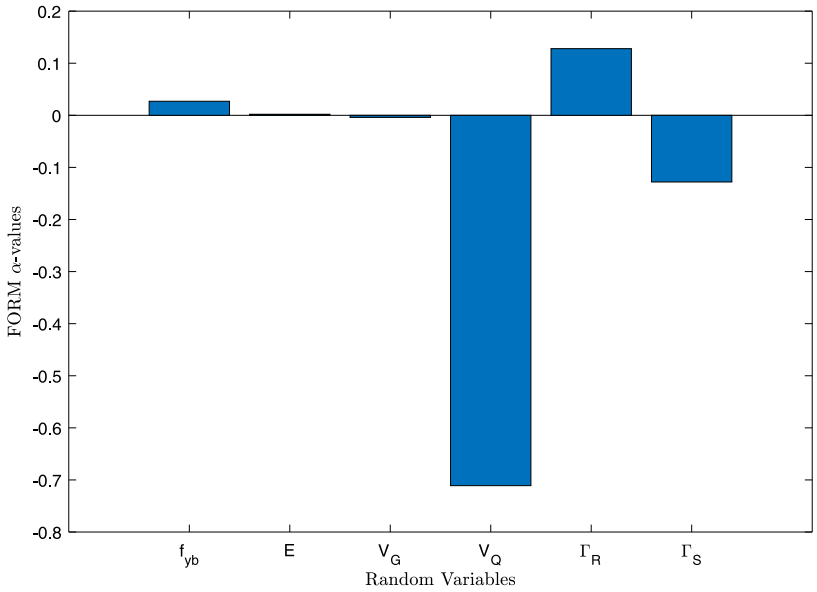

Fig. 10. Mean FORM importance vector α components for reliability analyses conducted using the modified EN 1993-1-3 model.

desirable because it can lead to cost-ineffective structures, contrary to the principles of reliability optimization embedded in structural design codes [45]. These observations align with findings from related studies that recommend cost-optimal design approaches amidst uncertainty [46–48].

Reducing the β values closer to β_T would imply a decrease in γ_{M0} below the typical baseline of 1.0, which is generally not favored due to the potential for underestimating the effects of uncertainties [49]. Therefore, we maintain γ_{M0} at 1.0 and propose the calibration of a modification factor k_γ in Eq. (22), aiming to achieve the specified reliability targets while also considering the effect of the load ratio κ. This approach is in line with the methodologies applied in recent reliability studies that employ modification factors for resistance models [50,51].

The modification factor k_γ modifies Eq. (1) as follows,

$$V_{b,Rd} = \frac{k_\gamma}{\gamma_{M0}} \cdot \frac{(h_w \cdot) \cdot t \cdot f_{bw}}{\sin(\phi)}. \tag{22}$$

To ensure that the revised expressions satisfy the designated reliability targets, the k_γ parameter is carefully adjusted. This adjustment is implemented to both the existing EN 1993-1-3 and its modified version. Typically, for structural components displaying ductile characteristics [52] and classified under Reliability Class 2 (RC2), a reliability target of $\beta_T = 3.8$ is advised, as per EN 1990 [17].

For the specific case of CFS channels under shear stress, it may be advisable to aim for a higher target reliability of $\beta_T = 4.3$, aligning with Reliability Class 3 (RC3). This is due to the potential instability risks, such as web buckling, associated with the thin walls of CFS channels. In the following, distinct values for the k_γ factor are calibrated and suggested, tailored for both the existing EN 1993-1-3 and its modified version. These adjustments are intended to ensure that these models meet the specified reliability targets of 3.8 and 4.3, corresponding to different ratios of variable to permanent actions denoted by κ.

Fig. 11 illustrates the relationship between the reliability index (β) at the 10% fractile and the proposed modification factor (k_γ), for various κ values ranging from 1.0 to 2.0 in increments of 0.5. The study particularly emphasizes the critical intersection where the line representing $\kappa = 2.5$ meets the prescribed reliability targets $\beta_T = 3.8$ for Reliability Class 2 (RC2) and $\beta_T = 4.3$ for Reliability Class 3 (RC3). At this point, based on the trend line analysis, the estimated k_γ values are identified to be approximately $k_\gamma = 1.5$ for RC2 and $k_\gamma = 1.3$ for RC3.

The potential threshold effect observed at $k_\gamma = 2.0$ for the EN 1993-1-3 model may indicate a physical limit in the material behavior or an inflection point within the resistance model that necessitates further investigation. This observation could be compared with findings from other studies exploring the behavior of CFS channels under varying load conditions and resistance modifications [53–55].

In the context of the modified EN 1993-1-3 (refer to Fig. 12), the estimated k_γ values are approximately $k_\gamma = 1.06$ for Reliability Class 2 (RC2) and $k_\gamma = 0.925$ for Reliability Class 3 (RC3). For the modified EN 1993-1-3 model, when considering the RC3 target β, the existing format in Eq. (1) remains applicable, but with a modification to the γ_{M0} value, changing it from 1.0 to 1.08.

Furthermore, in the case of the modified EN 1993-1-3, the change in the rate of β values with respect to the action ratios κ is not observed for the considered values of k_γ in Fig. 12. However, extrapolating the trend indicates that this significant value is likely to be greater than 1.25.

In conclusion, the calibration of k_γ based on the reliability targets of $\beta_T = 3.8$ and $\beta_T = 4.3$ provides a pathway to designs of CFS channels that meet both safety requirements and economic considerations [47].

6. Concluding synopsis

The study advances the understanding of reliability in shear design for CFS sections, evaluating both the existing and modified EN 1993-1-3 [12] models. Incorporating the FORM and MCS, key insights and recommendations are presented as follows:

- A substantial correlation is identified between the reliability index β and the relative web slenderness λ_w. This correlation is more pronounced in the original EN 1993-1-3 model, indicating enhanced reliability assessment in the modified version due to its inclusion of restraint levels in λ_w calculations.
- The modified EN 1993-1-3 model aligns more effectively with the reliability targets set forth by EN 1990, particularly for structures classified under RC2. The existing model tends to produce designs that are more conservative than necessary.
- Sensitivity analysis underscores the importance of precise parameter selection for reliability assessments, advocating for future design codes to incorporate considerations of restraint levels in λ_w calculations.

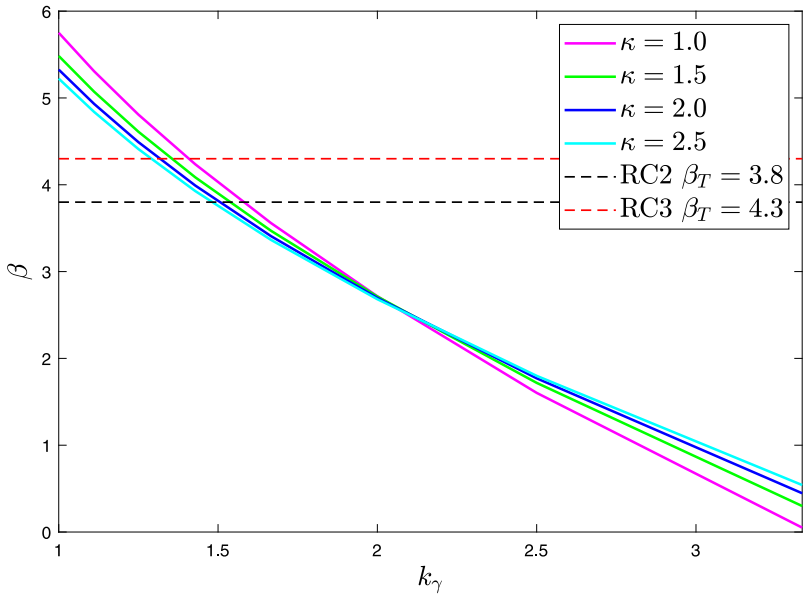

Fig. 11. 10% fractile of the reliability indices β as a function of k_γ for the EN 1993-1-3 model.

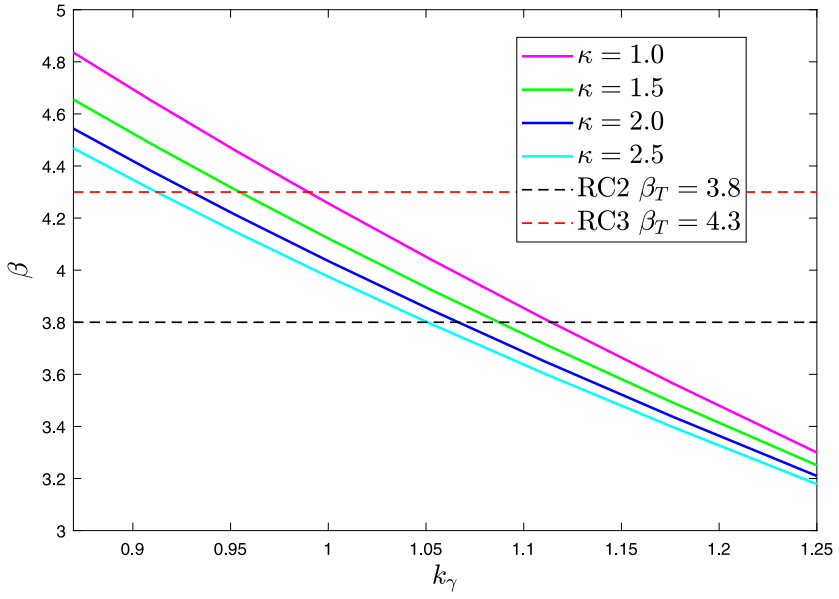

Fig. 12. 10% fractile of the reliability indices β as a function of k_γ for the modified EN 1993-1-3 model.

- It is recommended to maintain γ_{M0} at 1.0 and adjust the modification factor k_γ according to the load ratio κ, aiming to strike a balance between safety and economic efficiency.

In conclusion, the findings contribute to the enhancement of reliability in shear design of CFS sections, identify improvements for design standards, and propose solutions for balanced, economically viable designs and leveraging approaches endorsed by the JCSS. By adapting probabilistic models from hot-rolled steel, we address the lack of specific models for CFS sections, emphasizing the importance of considering material properties such as thickness in structural reliability analysis. Furthermore, our findings highlight the need for further research on the execution tolerances of thin-walled CFS sections to enhance structural performance and inform accurate design practices. These insights are anticipated to guide future revisions of design standards, fostering the development of resilient and cost-effective structural systems.

CRediT authorship contribution statement

L. Simwanda: Writing – review & editing, Writing – original draft, Software, Methodology, Investigation, Formal analysis, Data curation, Conceptualization. **P. Gatheeshgar:** Methodology, Investigation, Formal analysis, Data curation, Conceptualization, Writing – review & editing. **B.D. Ikotun:** Formal analysis, Investigation, Methodology, Project administration, Writing – review & editing. **M. Bock:** Formal analysis, Investigation, Methodology, Writing – review & editing. **E.K. Onyari:** Project administration, Resources, Writing – review & editing. **F.M. Ilunga:** Project administration, Writing – review & editing.

Declaration of competing interest

The authors declare that they have no known competing financial interests or personal relationships that could have appeared to influence the work reported in this paper.

Data availability

Data will be made available on request.

Acknowledgments

Recognition is given to the UQLab uncertainty quantification framework in Matlab [56], which served as an open-source platform for conducting the reliability analyses presented in this paper.

References

[1] P. Gatheeshgar, K. Poologanathan, S. Gunalan, I. Shyha, P. Sherlock, H. Rajanayagam, B. Nagaratnam, Development of affordable steel-framed modular buildings for emergency situations (covid-19), Structures 31 (2021) 862–875, http://dx.doi.org/10.1016/j.istruc.2021.02.004.

[2] R.A. LaBoube, Strength of cold-formed steel beam webs in bending, shear, and a combination of bending and shear, (Ph.D. thesis), Missouri University of Science and Technology, 1977, https://scholarsmine.mst.edu/doctoral_dissertations/367.

[3] P. Keerthan, M. Mahendran, New design rules for the shear strength of litesteel beams, J. Constr. Steel Res. 67 (2011) 1050–1063, http://dx.doi.org/10.1016/j.jcsr.2010.11.010.

[4] P. Keerthan, M. Mahendran, Improved shear design rules of cold-formed steel beams, Eng. Struct. 99 (2015) 603–615, http://dx.doi.org/10.1016/j.engstruct.2015.04.027.

[5] C.H. Pham, G.J. Hancock, Shear buckling of channels using the semi-analytical and spline finite strip methods, J. Constr. Steel Res. 90 (2013) 42–48, http://dx.doi.org/10.1016/j.jcsr.2013.07.019.

[6] C.H. Pham, G.J. Hancock, Shear buckling of thin-walled channel sections, J. Constr. Steel Res. 65 (2009) 578–585, http://dx.doi.org/10.1016/j.jcsr.2008.05.015.

[7] EN 1993-1-3, eurocode 3: Design of steel structures - part 1-3: General rules - supplementary rules for cold-formed members and sheeting, 2006.

[8] AISI-S100, North American Specification for the Design of Cold-Formed Steel Structural Members, American Iron and Steel Institute, 2001.

[9] AS/NZS-4600 Australian/new zealand standard cold-formed steel structures, 2018.

[10] Cao Hung Pham, Gregory J. Hancock, Direct strength design of cold-formed C-sections for shear and combined actions, J. Struct. Eng. 138 (6) (2012) 769–778, http://dx.doi.org/10.1061/(ASCE)ST.1943-541X.0000510.

[11] B. Schafer, T. Peköz, The behavior and design of longitudinally stiffened thin-walled compression elements, Thin-Walled Struct. 27 (1997) 65–78, http://dx.doi.org/10.1016/0263-8231(96)00016-X.

[12] P. Gatheeshgar, M. Bock, D. Chandrasiri, T. Suntharalingam, Assessment of eurocode shear design provisions for cold-formed steel sections, Structures 47 (2023) 2066–2073, http://dx.doi.org/10.1016/j.istruc.2022.12.017.

[13] I.A. Chaves, A.T. Beck, M. Malite, Reliability-based evaluation of design guidelines for cold-formed steel-concrete composite beams, J. Brazilian Soc. Mech. Sci. Eng. 32 (2010) 442–449, http://dx.doi.org/10.1590/S1678-58782010000500003.

[14] V. Meimand, B. Schafer, Impact of load combinations on structural reliability determined from testing cold-formed steel components, Struct. Saf. 48 (2014) 25–32, http://dx.doi.org/10.1016/j.strusafe.2013.10.006.

[15] B. Ellingwood, T.V. Galambos, Probability-based criteria for structural design, Struct. Saf. 1 (1982) 15–26, http://dx.doi.org/10.1016/0167-4730(82)90012-1.

[16] Structural reliability under combined random load sequences, Comput. Struct. 9 (1978) 489–494, http://dx.doi.org/10.1016/0045-7949(78)90046-9.

[17] EN 1990, eurocode 0: Basis of structural design, 2002.

[18] International Organization for Standardization, ISO 2394:2015 - general principles on reliability for structures, 2015, http://dx.doi.org/10.1007/s11367-011-0297-3.

[19] S.C. Lee, J.S. Davidson, C.H. Yoo, Shear buckling coefficients of plate girder web panels, Comput. Struct. 59 (1996) 789–795, http://dx.doi.org/10.1016/0045-7949(95)00325-8.

[20] M. Holickỳ, J.V. Retief, M. Sỳkora, Assessment of model uncertainties for structural resistance, Probab. Eng. Mech. 45 (2016) 188–197, http://dx.doi.org/10.1016/j.probengmech.2015.09.008.

[21] M. Sykora, M. Holicky, M. Prieto, P. Tanner, Uncertainties in resistance models for sound and corrosion-damaged rc structures according to en 1992-1-1, Mater. Struct. 48 (2015) 3415–3430, http://dx.doi.org/10.1617/s11527-014-0409-1.

[22] P. Keerthan, M. Mahendran, Experimental studies on the shear behaviour and strength of litesteel beams, Eng. Struct. 32 (2010) 3235–3247, http://dx.doi.org/10.1016/j.engstruct.2010.06.012.

[23] P. Keerthan, M. Mahendran, Experimental investigation and design of lipped channel beams in shear, Thin-Walled Struct. 86 (2015) 174–184, http://dx.doi.org/10.1016/j.tws.2014.08.024.

[24] C.H. Pham, G.J. Hancock, Experimental investigation of high strength cold-formed c-sections in combined bending and shear, J. Struct. Eng. 136 (2010) 866–878, http://dx.doi.org/10.1061/(ASCE)ST.1943-541X.0000172.

[25] B. Chen, K. Roy, Z. Fang, A. Uzzaman, C.H. Pham, G.M. Raftery, J.B. Lim, Shear capacity of cold-formed steel channels with edge-stiffened web holes, unstiffened web holes, and plain webs, J. Struct. Eng. 148 (2022) 04021268, http://dx.doi.org/10.1061/(ASCE)ST.1943-541X.0003250.

[26] S.H. Pham, C.H. Pham, G.J. Hancock, Experimental study of shear strength of cold-formed channels with an aspect ratio of 2.0, J. Constr. Steel Res. 149 (2018) 141–152, http://dx.doi.org/10.1016/j.jcsr.2018.07.002.

[27] S.H. Pham, C.H. Pham, C.A. Rogers, G.J. Hancock, Experimental validation of the direct strength method for shear spans with high aspect ratios, J. Constr. Steel Res. 157 (2019) 143–150, http://dx.doi.org/10.1016/j.jcsr.2019.02.018.

[28] N. Smirnov, Table for estimating the goodness of fit of empirical distributions, Ann. Math. Stat. (1948).

[29] A. Kolmogorov, Sulla Determinazione Empirica Di Una Legge Di Distribuzione, Giornale dell'Istituto Italiano degli Attuari, 1933.

[30] F.J. Massey Jr., The kolmogorov-smirnov test for goodness of fit, J. Amer. Statist. Assoc. (1951).

[31] H.W. Lilliefors, On the kolmogorov-smirnov test for normality with mean and variance unknown, J. Amer. Statist. Assoc. (1967).

[32] L.H. Miller, Table of percentage points of kolmogorov statistics, J. Amer. Statist. Assoc. (1956).

[33] S. Siegel, Nonparametric Statistics for the Behavioral Sciences, McGraw-Hill, 1956.

[34] W.J. Conover, Practical Nonparametric Statistics, John Wiley & Sons, 1971.

[35] K. Pearson, On the criterion that a given system of deviations from the probable in the case of a correlated system of variables is such that it can be reasonably supposed to have arisen from random sampling, Philos. Mag. Series (1900).

[36] R.A. Fisher, Statistical Methods for Research Workers, Oliver and Boyd, Edinburgh, 1925.

[37] JCSS, joint committee on structural safety probabilistic model code part 3: Resistance models, 2001.

[38] C.J. Turkstra, Theory of Structural Design Decisions Study No. 2, Solid Mechanics Division, University of Waterloo, Ontario, Canada, 1970.

[39] G.W. Parry, The characterization of uncertainty in probabilistic risk assessments of complex systems, Reliab. Eng. Syst. Saf. 54 (1996) 119–126, http://dx.doi.org/10.1016/S0951-8320(96)00069-5.

[40] A.S. Nowak, M.M. Szerszen, Calibration of design code for buildings (aci 318): Part 1—statistical models for resistance, Struct. J. 100 (2003) 377–382, http://dx.doi.org/10.14359/12613.

[41] BS EN 1991, uk national annex to eurocode 1: Actions on structures - part 1-1: General actions - densities, self-weight, imposed loads for buildings, 2005.

[42] A.M. Hasofer, N.C. Lind, Exact and invariant second-moment code format, J. Eng. Mech. Div. 100 (1974) 111–121, http://dx.doi.org/10.1061/JMCEA3.0001848.

[43] A.H.-S. Ang, W.H. Tang, Probability concepts in engineering planning and design: Volume ii decision, risk, and reliability, 1984.

[44] R. Melchers, Structural reliability analysis and prediction, 1999.

[45] Y. Aoues, A. Chateauneuf, Benchmark study of numerical methods for reliability-based design optimization, Struct. Multidiscipl. Optim. 41 (2010) 277–294, http://dx.doi.org/10.1007/s00158-009-0412-2.

[46] M. Baravalle, Risk and Reliability Based Calibration of Structural Design Codes: Principles and Applications (Doctoral thesis), Norwegian University of Science and Technology (NTNU, 2017, Available at: http://hdl.handle.net/11250/2485103.

[47] N. Gayton, A. Mohamed, J.D. Sorensen, M. Pendola, M. Lemaire, Calibration methods for reliability-based design codes, Struct. Saf. 26 (2004) 91–121, http://dx.doi.org/10.1016/S0167-4730(03)00024-9.

[48] P. Nuzzo, N. Bajaj, M. Masin, D. Kirov, R. Passerone, A.L. Sangiovanni-Vincentelli, Optimized selection of reliable and cost-effective safety-critical system architectures, IEEE Trans. Comput.-Aided Des. Integr. Circuits Syst. 39 (2019) 2109–2123, http://dx.doi.org/10.1109/TCAD.2019.2963255.

[49] R. Caspeele, K. Van Den Hende, Validation of the harmonized partial factor method for design and assessment of concrete structures as proposed for fib model code 2020, Struct. Concr. 24 (2023) 4368–4376, http://dx.doi.org/10.1002/suco.202201109.

[50] V. Mohsenian, S. Padashpour, I. Hajirasouliha, Seismic reliability analysis and estimation of multilevel response modification factor for steel diagrid structural systems, J. Build. Eng. 29 (2020) 101168, http://dx.doi.org/10.1016/j.jobe.2019.101168.

[51] B. Smith, S. Arwade, B. Schafer, C. Moen, Design component and system reliability in a low-rise cold formed steel framed commercial building, Eng. Struct. 127 (2016) 434–446, http://dx.doi.org/10.1016/j.engstruct.2016.08.049.

[52] A. Masoud Hassanzadeh, M. Dehestani, H. Nazarpour, Reliability analysis of flexural provisions of frp-rc beams and sensitivity analysis based on form, Eng. Struct. 285 (2023) 116037, http://dx.doi.org/10.1016/j.engstruct.2023.116037.

[53] J. Zhu, L.-Y. Li, Effect of shear stress on distortional buckling of cfs beams subjected to uniformly distributed transverse loading, mechanics of advanced, Mater. Struct. 26 (2019) 1423–1429, http://dx.doi.org/10.1080/15376494.2018.1432798.

[54] N. Degtyareva, P. Gatheeshgar, K. Poologanathan, S. Gunalan, M. Lawson, P. Sunday, Combined bending and shear behaviour of slotted perforated steel channels: Numerical studies, J. Constr. Steel Res. 161 (2019) 369–384, http://dx.doi.org/10.1016/j.jcsr.2019.07.008.

[55] P. Gatheeshgar, K. Poologanathan, S. Gunalan, I. Shyha, K.D. Tsavdaridis, M. Corradi, Optimal design of cold-formed steel lipped channel beams: Combined bending, shear, and web crippling, in: Structures, vol. 28, Elsevier, 2020, pp. 825–836, http://dx.doi.org/10.1016/j.istruc.2020.09.027.

[56] S. Marelli, B. Sudret, Uqlab: A framework for uncertainty quantification in matlab, in: Vulnerability, Uncertainty, and Risk, American Society of Civil Engineers, Reston, VA, 2014, pp. 2554–2563, http://dx.doi.org/10.1061/9780784413609.257.